

**Supplementary Information**

**$\text{KLa}_{(0.95-x)}\text{Gd}_x\text{F}_4:\text{Eu}^{3+}$  hexagonal phase nanoparticles as luminescent probe for  
*in-vitro* Huh-7 cancer cell imaging**

Mohini Gupta<sup>a,b\*</sup>, Rajamani Nagarajan<sup>b</sup>, CH. Ramamurthy<sup>c</sup>, Perumal Vivekanandan<sup>c</sup>, G. Vijaya

Prakash<sup>a\*</sup>

<sup>a</sup>Nanophotonics Lab, Department of Physics, Indian Institute of Technology Delhi, New Delhi,  
110016 INDIA

<sup>b</sup>Materials Chemistry Group, Department of Chemistry, University of Delhi, Delhi 110007  
INDIA

<sup>c</sup>Kusuma School of Biological Sciences, Indian Institute of Technology Delhi, New Delhi,  
110016, INDIA

**Supporting Table S1.** Crystallographic data of hexagonal  $\text{KLa}_{(0.95-x)}\text{Gd}_x\text{F}_4:5\%\text{Eu}^{3+}$  ( $x = 0.4$ ) nanocrystals.

<b>Formula</b>	$(\text{KLaF}_4)_{1.5}$
<b>Crystal Structure</b>	Hexagonal
<b>space group</b>	$\text{P}\bar{6}2\text{m}$ (#189)
<b>a (Å)</b>	6.5766(5)
<b>c (Å)</b>	3.7964(2)
<b>V (Å<sup>3</sup>)</b>	142.20(1)
<b><math>\rho_{\text{calc}}</math> (g/cm<sup>3</sup>)</b>	4.42(5)
<b><math>R_{\text{exp}}</math> (%)</b>	4.27
<b><math>R_{\text{p}}</math> (%)</b>	5.69
<b><math>R_{\text{wp}}</math> (%)</b>	7.69
<b>GOF (S)</b>	1.86

**Supporting Table S2.** Refined positional parameters for hexagonal  $\text{KLa}_{(0.95-x)}\text{Gd}_x\text{F}_4:5\%\text{Eu}^{3+}$  ( $x = 0.4$ ) nanocrystals after the final cycle of refinement.

Refined unit cell parameters  $a$  (Å) = 6.5766(5) and  $c$  (Å) = 3.7964(2)

<b>Atom</b>	<b>Site</b>	<b>SOF</b>	<b>x/a</b>	<b>y/b</b>	<b>z/c</b>	<b><math>B_{\text{eq}}</math></b>
La1/Eu1/Gd1	1a	0.57/0.05/0.38	0	0	0	1.0
K1/La2	2d	0.72438/0.27562	1/3	2/3	1/2	1.0
F1	3g	1.0	0.63044	0	0	1.0
F2	3f	1.0	0.21410	0.49751	1/2	1.0

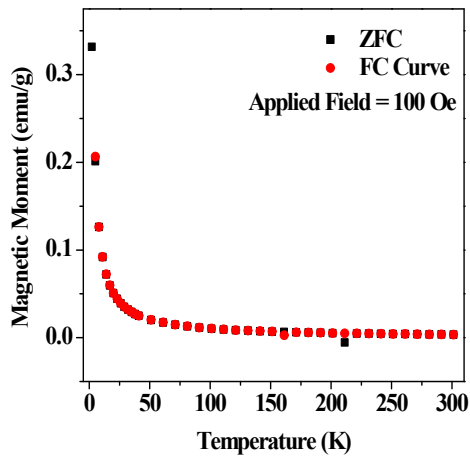


**Figure S1:** ZFC-FC curves collected at 100 Oe magnetic field for  $\text{KLa}_{(0.95-x)}\text{Gd}_x\text{F}_4:5\%\text{Eu}^{3+}$  ( $x = 0.4$ ) nanorods.

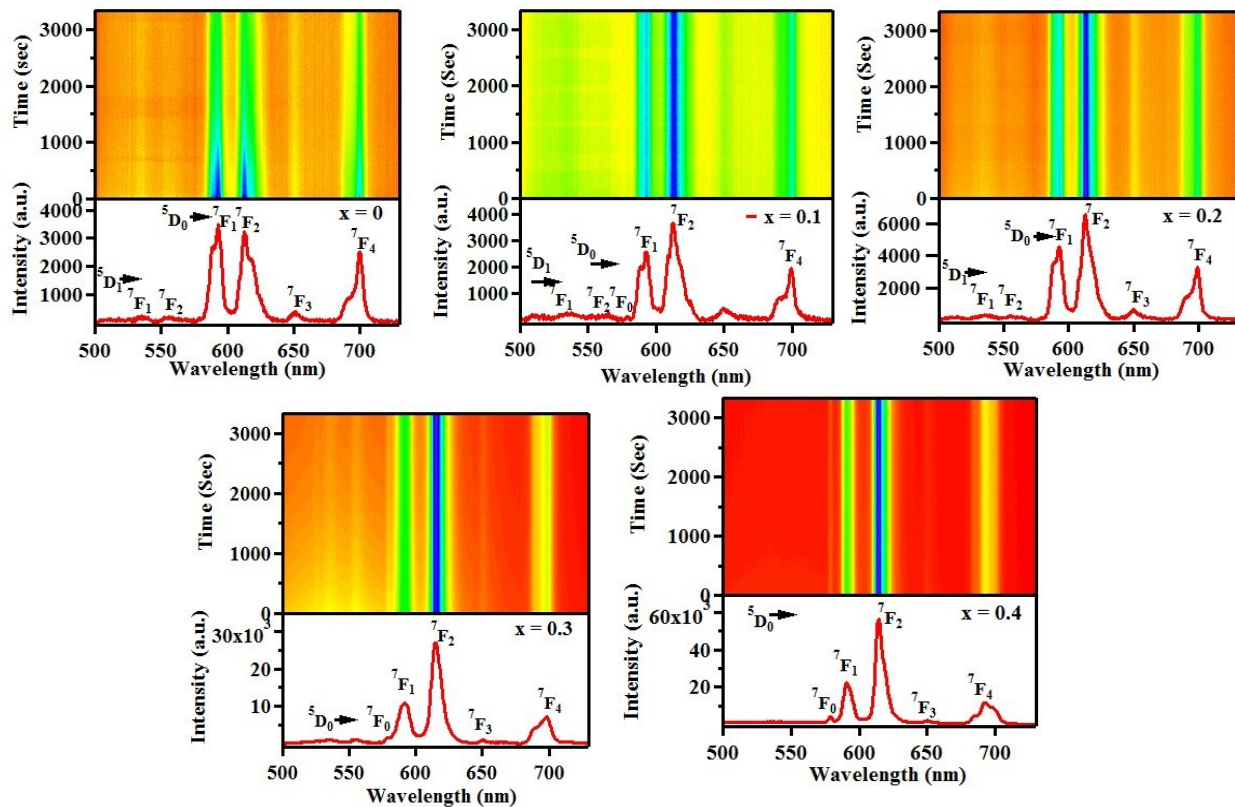


**Figure S2.** Longer exposure time scans and respective PL spectra under 405 nm laser excitation of  $\text{KLa}_{0.95-x}\text{Gd}_x\text{F}_4:5\%\text{Eu}^{3+}$  ( $x=0$  to  $0.4$ ).

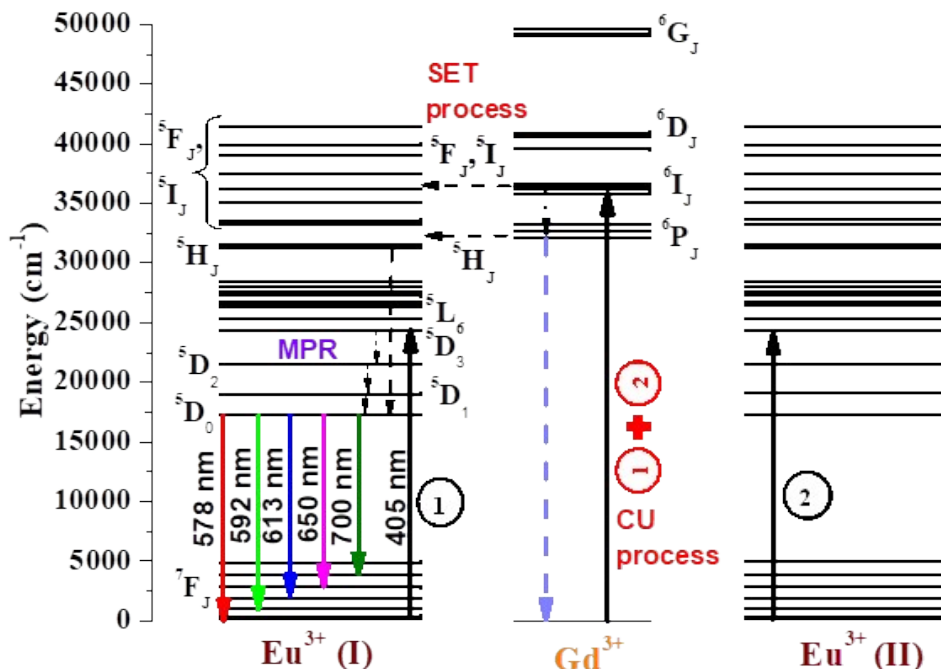


**Figure S3.** Sketch of possible energy transitions in Gd - Eu doped samples.

From the Dieke energy level scheme (Figure S3), under 405 nm excitation,  $Gd^{3+}$  ion can't be activated unlike 273 nm excitation and energy transfer from  $Gd \rightarrow Eu$  is not possible. However, it is observed that PL intensity, broadening and no. of splitting of peaks corresponding to transitions  ${}^5D_0 \rightarrow {}^7F_2$  and  ${}^5D_0 \rightarrow {}^7F_4$  increases with increment of  $Gd^{3+}$  concentration to  $x=0.4$  at 405 nm laser excitation while Eu concentration is fixed (Figure 3(a)). This PL enhancement can be explained by combine effect of the co-operative upconversion (CU) and the successive energy transfer (SET) processes.<sup>1</sup> General mechanism involved in  $Eu^{3+}$  emission is, absorption of 405 nm incident light through  ${}^7F_0 \rightarrow {}^5D_3$  (energy  $24335 \text{ cm}^{-1}$ ) transition, this energy is transited to  ${}^5D_0$  by non-radiative transition and finally visible emission lines occur through  ${}^5D_0 \rightarrow {}^7F_J$  transitions. With the  $Gd^{3+}$  dopant,  $KLa_{1-x}Gd_xF_4:Eu^{3+}$  nanoparticles could accept energy from two excited  $Eu^{3+}$  ( ${}^5D_3$ ) ions via CU process. Therefore, this energetically active  $Gd^{3+}$  ion may be excited to higher energy levels ( ${}^8S_{7/2} \rightarrow {}^6P_J$ ,  ${}^6I_J$ ,  ${}^6G_J$ ). Back energy transfer via SET process from Gd to Eu

takes place and energy of activated  $\text{Eu}^{3+}$  ion matched with energy of  ${}^6\text{G}_7$  energy state of  $\text{Gd}^{3+}$ . Finally,  $\text{Eu}^{3+}$  emission lines are generated through radiative transitions from  ${}^4\text{H}_J \rightarrow {}^5\text{D}_0 \rightarrow {}^7\text{F}_J$  ( $J=0$  to 4). Therefore, CU and SET process with minimal energy loss play important role in enhancement of PL intensity after doping of  $\text{Gd}^{3+}$  ions in fluoride nanocrystals.

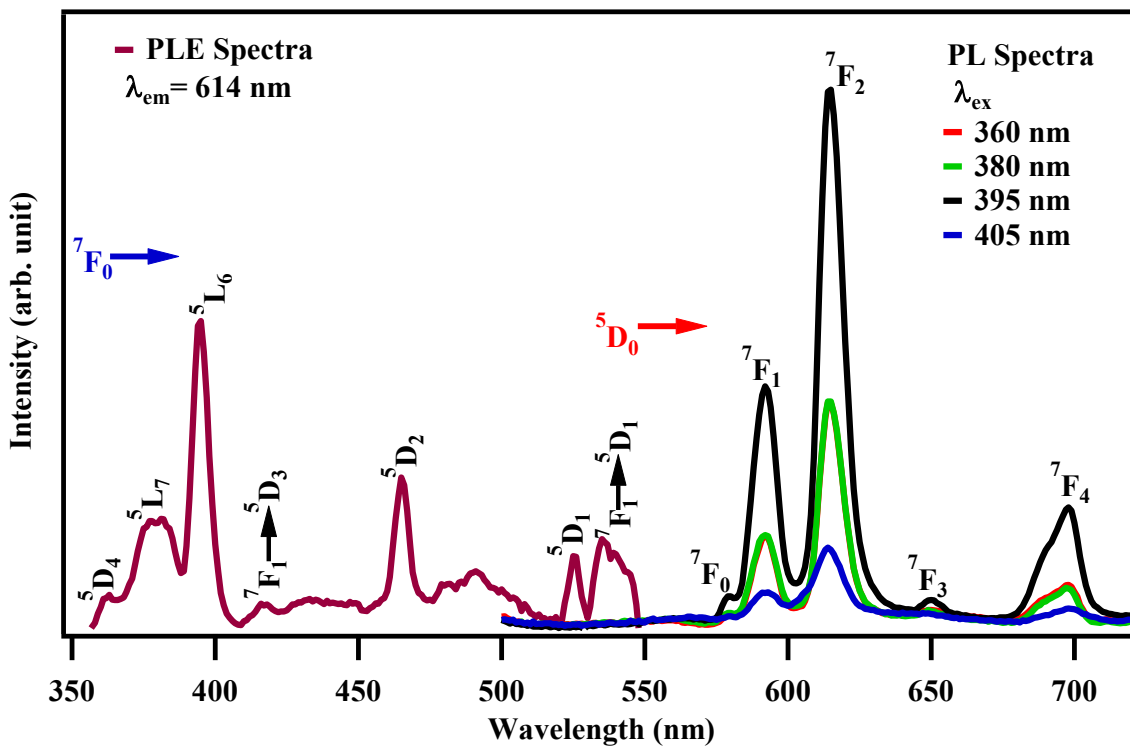


**Figure S4.** Photoluminescence excitation (PLE) spectra at  $\lambda_{\text{em}} = 614 \text{ nm}$  ( ${}^5\text{D}_0 \rightarrow {}^7\text{F}_2$ ) and Emission spectra at different excitation wavelength recorded for  $\text{KLa}_{(0.95-x)}\text{Gd}_x\text{F}_4:5\%\text{Eu}^{3+}$  ( $x = 0.4$ ) nanoparticles.

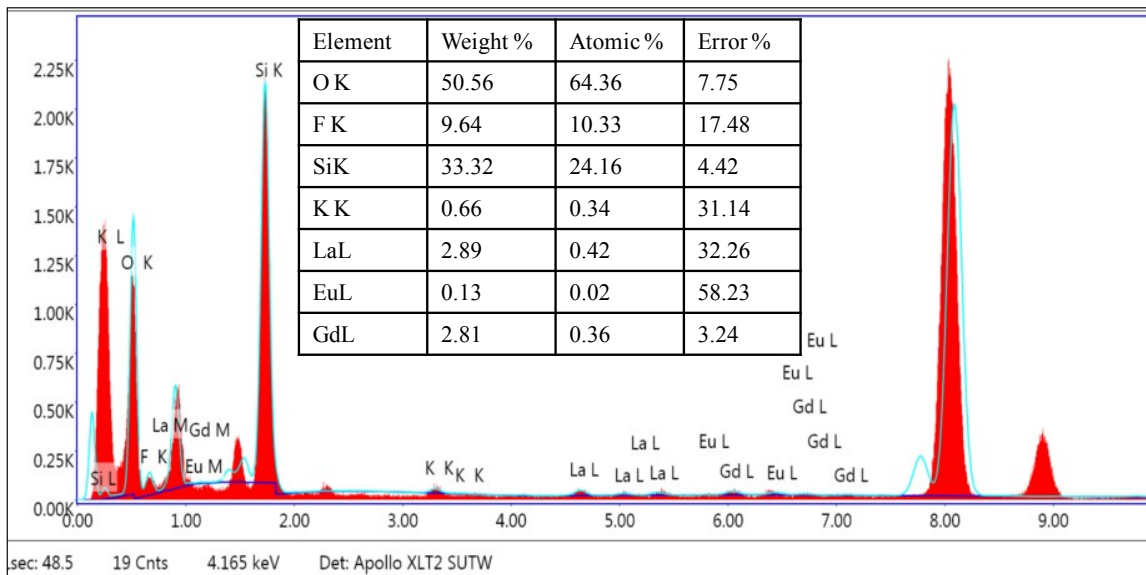


**Figure S5.** EDS analysis of silica/oleic acid coated  $\text{KLa}_{(0.95-x)}\text{Gd}_x\text{F}_4:5\%\text{Eu}^{3+}$  ( $x = 0.4$ ) nanorods.

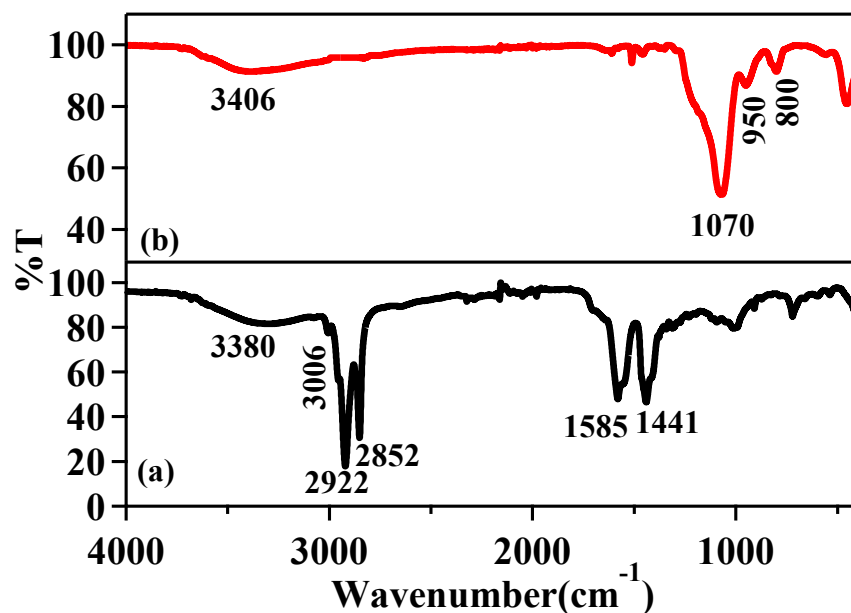


**Figure S6.** FT-IR data for (a) oleic acid (b) oleic acid/silica capped  $\text{KLa}_{(0.95-x)}\text{Gd}_x\text{F}_4:5\%\text{Eu}^{3+}$  ( $x = 0.4$ ) nanocrystals.

In the OA capped nanoparticles, the band centered at  $3006 \text{ cm}^{-1}$  is ascribed to the  $=\text{C-H}$  stretching band. The asymmetric ( $\nu_{\text{as}}$ ) and symmetric ( $\nu_{\text{s}}$ )  $\text{CH}_2$  stretching bands are present at  $2922$  and  $2852 \text{ cm}^{-1}$  that confirms assimilation of oleic acid molecules on the surface of

nanoparticles. The transmission bands centered at 1539 and 1440  $\text{cm}^{-1}$  are attributed to the asymmetric ( $\nu_{\text{as}}$ ) and symmetric ( $\nu_{\text{s}}$ )  $\text{COO}^-$  stretching vibrations. After the silica modification, characteristic bands of OA completely disappeared and a broad band at 3406  $\text{cm}^{-1}$  corresponds to O-H stretching vibration appeared. The silica capping on the surface of nanoparticles is confirmed by the presence of symmetric Si-O-Si strong and broad band at 1070  $\text{cm}^{-1}$ . The Si-OH and asymmetric  $\text{SiO}_4$  stretching bands are present at 950 and 800  $\text{cm}^{-1}$ .

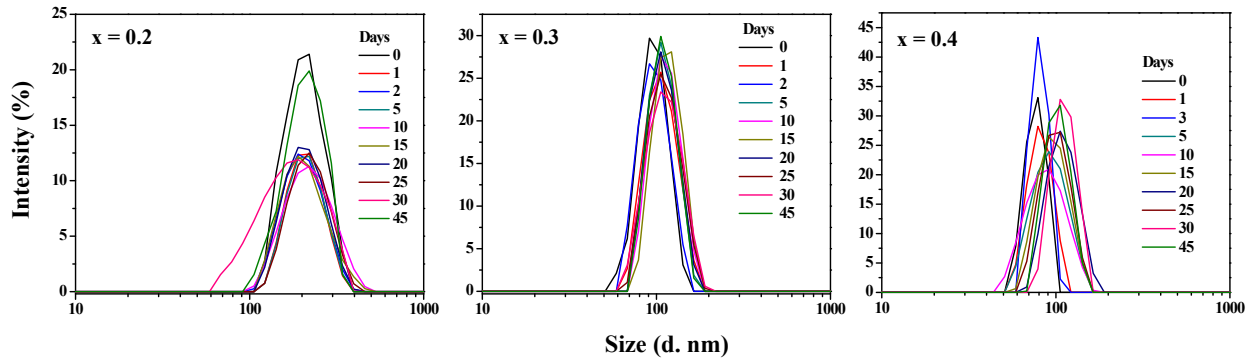


**Figure S7.** DLS data for  $\text{KLa}_{(0.95-x)}\text{Gd}_x\text{F}_4:5\%\text{Eu}^{3+}$  ( $x = 0.2 - 0.4$ ) samples collected at different time scales.

### Diffusion dominated aggregation model

The experimental long-term stability data are scaled by aggregation and fragmentation theory based on modified Smoluchowski rate equation. According to this model,

The time evolution of  $P(k, t)$ , where  $P(k, t)$  is called the probability of forming a cluster of comprising  $k$  particles at time  $t$ , is expressed by equations

$$\frac{dP(k, t)}{dt} = \sum_{i+j=k} K_{ij} P(i, t) P(j, t) - P(k, t) \sum_{j=1}^{\infty} K_{kj} P(j, t) + \omega P(k+1, t) - \omega P(k, t), \quad k > 1 \quad (1)$$

$$\frac{dP(1, t)}{dt} = -P(1, t) \sum_{j=1}^{\infty} K_{kj} P(j, t) + \omega \sum_{j=2}^{\infty} P(j, t), \quad k = 1 \quad (2)$$

Where aggregation kernel  $K_{ij} = D (i^{-\mu} + j^{-\mu})$  represents the rate of integration of a cluster of size  $i$  with cluster of size  $j$  that make a bigger cluster of size  $k = i + j$ . Here  $D$  is attributed to the forming of a large cluster due to the aggregation of monomers, while the loss or fragmentation of a particle from its parent aggregate is represented by  $\omega$ . The diffusivity  $\mu$  of cluster  $k$  is classified as (1)  $\mu = 0$ , mass independent mobility, the different size clusters diffuses with equal mobility, (2)  $\mu \neq 0$ , mobility of larger clusters are slow and results slower growth rate if aggregates. (3)  $\mu = \infty$ , in this condition, only monomers perform Brownian motion.

The first and third terms in equations (1) and (2) counted as gain term due to the formation of clusters of size  $k$ , while second and fourth terms are called loss term due to the fragmentation of clusters of size  $k$ . The condition of steady state is defined as  $\partial P(k,t)/\partial t = 0$ . Based on this theory, the growth rate ( $\beta$ ) of aggregates at intermediate time scale is governed by a power law as

$$\langle k(t) \rangle \sim t^\beta.$$

## References

1. Y. Xie, W. He, F. Li, T. S. H. Perer, L. Gan, Y. Han, X. Wang, S. Li, H. Dai, Luminescence enhanced  $\text{Eu}^{3+}/\text{Gd}^{3+}$  co-doped hydroxyapatite nanocrystals as imaging agents in vitro and in vivo, ACS Appl. Mater. Interfaces, **2016**, 8, 16, 10212–10219.